JOURNAL OF CATALYSIS 67, 145–158 (1981)

ESR Studies on Hydrodesulfurization Catalysts: Nickel- or Cobalt-Promoted Sulfided Tungsten- or Molybdenum-Containing Catalysts

A. J. A. KONINGS, W. L. J. BRENTJENS, D. C. KONINGSBERGER, AND V. H. J. DE BEER

Laboratory for Inorganic Chemistry, Eindhoven University of Technology, P.O. Box 513, 5600 MB Eindhoven, The Netherlands

Received March 5, 1980; revised July 15, 1980

ESR spectra of nickel- or cobalt-promoted sulfided tungsten- or molybdenum-containing catalysts are measured together with the influence of equilibration at different H_2S/H_2 ratios and CO adsorption hereon. The ESR measurements are compared with thiophene hydrodesulfurization (HDS) activities. The influence of nickel and cobalt on the ESR spectra is essentially the same. This similarity also holds for the thiophene HDS activities. A new signal VI ($g = 2.06$, $\Delta H = 220$ G for Ni–Mo; $g = 2.08$, $\Delta H = 220$ G for Ni–W) not occurring in unpromoted catalysts is detected. The intensities of signals II, III, IV, and VI are dependent on the composition of the interacting atmosphere. The results are discussed in terms of $WS_2(MoS_2)$ crystallite edge decoration with promotor ions. Possible surface configurations corresponding with the different paramagnetic sites are described.

INTRODUCTION

It is widely accepted by now that the catalytic active phase of the intensively applied hydrodesulfurization catalyst systems consists of $MoS_2(WS_2)$ crystallites (*1, 2*). The catalytic activity can be enhanced (promoted) by nickel or cobalt, often referred to as promoter ions. It is the role of these promotor ions that is still not well understood. Several models have been proposed. The basic idea of the intercalation model (pseudointercalation or decoration seems to describe the proposed interaction better) from Farragher and Cossee (*3*) is the incorporation of promotor ions in octahedral holes between the MS_2 layers, restricted to the crystal edges. The reorganization of the surface due to this incorporation should lead to an increase of active sites. The model based on synergy by contact proposed by Delmon and coworkers (*4*) describes the promotor action as an electron transfer between surfaces of $MoS_2(WS_2)$ and $Co_9S_8(Ni_3S_2)$ crystallites.

Surface W^{3+} (Mo^{3+}) ions connected with anion vacancies play the role of the catalytic active centers in the decoration model. Since W^{3+} ions are paramagnetic, ESR can be used to study the active centers. The ESR results obtained at our laboratory for the unpromoted tungsten- or molybdenum-containing catalysts have been reported earlier (*5*). The necessity of measuring sulfided catalysts *in situ* has been demonstrated (*5, 6*). Five different signals could be analyzed in the ESR spectra of these catalysts. Signal I (oxo-Mo^{5+}, $g = 1.933$, and oxo-W^{5+}, $g = 1.78$) and possibly signal III arise as a result of interactions with the support. Three other signals originate from the disulfide phase. Signal II ($g = 1.985$ for Mo and $g = 1.91$ for W) and signal IV ($g = 2.01$ for W) show a complementary behavior upon evacuation and H_2S adsorption and are therefore ascribed to paramagnetic surface species. It has been attempted to assign signals II and IV to surface M^{3+} or M^{5+} ions with different sulfur ligand symmetries. The origin of another signal (V) remained unexplained but it might be re-

0021-9517/81/010145-14$02.00/0

lated with the presence of bulk defect structures.

In the present study the influence of the promotor ions upon the paramagnetic species mentioned above will be demonstrated for the systems Ni(Co)–W(Mo)/SiO_2(γ-Al_2O_3). Spectra of cobalt-promoted alumina-supported catalysts are not shown since the signal originating from Co^{2+} ions in the support interferes with the signals from the disulfide phase. For a few tungsten-containing catalysts the effect of variations in the H_2S/H_2 ratio (equilibration) as well as carbon monoxide adsorption will be demonstrated.

The system Ni–W has been studied earlier by Voorhoeve (*7*). He reported a correlation between benzene hydrogenation activity and intensity of an ESR signal most probably identical to our signal IV (*5*). Probably due to catalyst pretreatment (sulfidation procedure) the intensities of signals II and V are low in his samples.

The drastic change in g-value and the decrease in number of paramagnetic species upon introduction of promotor ions found in the present study will be discussed in terms of surface reorganization caused by these promotor ions.

EXPERIMENTAL

Catalyst Preparation

All starting materials were free from interfering paramagnetic impurities.

Silica-supported catalysts. SiO_2 (Ketjen F-2) was successively washed with excess ammonia (4.5 *N*) and distilled water. After drying at 383 K for 16 hr it was calcined in air at 873 K for 2.5 hr. The pore volume was then 1.05 $cm^3\ g^{-1}$ and the surface area 400 $m^2\ g^{-1}$. Aqueous solutions of analytical-grade ammonium heptamolybdate (Merck), ammonium metatungstate (Koch–Light Laboratories Ltd.), nickel nitrate (BDH), or cobalt nitrate (Merck) were used for pore volume impregnation. Silica was first impregnated with ammonium heptamolybdate or ammonium metatungstate, dried 16 hr at 383 K, calcined in air 16 hr at 773 K, and sulfided under standard conditions described below.

Then nickel or cobalt was introduced, followed by drying for 16 hr at 383 K and the standard sulfiding procedure. This "double" sulfiding was used for silica-supported samples to prevent the formation of cobalt or nickel molybdates or tungstates (*8*).

Alumina-supported catalysts. γ-Al_2O_3 was prepared by calcining boehmite (Martinswerk GmbH) in air for 2 hr at 873 K. The pore volume was then 0.35 $cm^3\ g^{-1}$ and the surface area 215 $m^2\ g^{-1}$. The same aqueous solutions as mentioned above were used for pore volume impregnation. First alumina was impregnated with ammonium heptamolybdate or ammonium metatungstate, dried 16 hr at 383 K, calcined in air at 773 K, then nickel nitrate solution was added, followed by drying 16 hr at 383 K, and calcining 16 hr at 773 K in air. Finally the catalyst was sulfided under standard conditions.

Sulfiding Procedure

Catalysts samples (200 mg) were treated in H_2 containing 16% (v/v) H_2S at a flow rate of 50 $cm^3\ min^{-1}$ and using the following temperature program: 10 min 295 K, linear increase from 295 to 673 K in 260 min, 20 hr 673 K, quenching to 295 K. It has been demonstrated (*5, 6*) that the properties of sulfided catalysts change upon exposure to oxygen. We therefore used a special ESR reactor to prevent contamination of the sample by oxygen (*5*). Hydrogen was deoxygenated over BTS catalyst (BASF R3-11) and dried over molecular sieves (Union Carbide 4A). Hydrogen sulfide (Matheson CP grade) was used as supplied.

Equilibration Procedure

Tungsten and nickel–tungsten-containing catalysts were treated with hydrogen containing 1 or 0.01% (v/v) H_2S, at 673 K for 24 hr, immediately after the standard sulfiding procedure was completed. These

samples were then quenched to 295 K and measured under the H_2S/H_2 atmosphere as used for equilibration. The H_2S/H_2 gas mixtures (Air Liquide) containing H_2S of 99% and H_2 of 99.9999% purity were used without further purification. The composition of these gas mixtures was checked frequently during each equilibration experiment.

Carbon Monoxide Adsorption

Freshly sulfided W(19.3)/SiO_2 and Ni(4)–W(19.3)/SiO_2 samples (numbers in parentheses are wt% NiO and WO_3, respectively) were evacuated ($<10^{-3}$ Torr, 295 K) and contacted with 40 Torr CO (10 min at 295 K and 15 min at 473 K). ESR spectra were recorded after each treatment (sulfiding, evacuation, CO at 295 K, and CO at 473 K). Carbon monoxide (Matheson CP grade) was used as supplied.

ESR Measurements

The ESR measurements were carried out using a Varian E-15 spectrometer equipped with a TE 104 dual-sample cavity. A Varian Strong Pitch sample ($g = 2.0028$, 3×10^{15} spins cm^{-1}) was used to calibrate the magnetic field, and functioned as a standard for the quality factor of the ESR cavity. Accuracy of the calculated relative and absolute signal intensities was 10 and 25%, respectively. In order to determine signal intensities as accurately as possible, ESR spectra were recorded in the temperature range 20–100 K (in a few cases 4–300 K) by means of a liquid-helium continuous-flow cryostat (Oxford Instruments).

HDS Activity Measurements

Thiophene conversion measurements were performed at atmospheric pressure and 673 K in a continuous-flow reactor (*9*). Catalyst (200 mg) was presulfided with H_2 containing 16% (v/v) H_2S at a flow rate of 50 cm^3 min^{-1}, using the following temperature program: 10 min 295 K, linear temperature increase from 295 to 673 K in 1 hr, 2 hr 673 K. Then the gas mixture was changed to H_2 with 7% (v/v) thiophene, 50 cm^3 min^{-1}. Thiophene HDS and butene hydrogenation data were obtained with stabilized (2-hr run) catalysts. Although the sulfiding procedure differs from the one used to prepare samples for ESR measurements it is believed that the obtained activities are at least indicative for their sequence to one another.

RESULTS

ESR Spectra

The various ESR signals that we have detected in sulfided catalysts are displayed in Figs. 1–6 (measured at 20 K). They are indicated by arrows at the approximate position of their low-field peaks which are found to be better resolved than the high-field peaks (*5*). Only those low-field peaks which are clearly observable are indicated. Since the signals show considerable overlap, it is difficult to determine the ESR parameters of each signal accurately. The g-value and linewidth for those signals that could be detected separately, are tabulated in Table 1. In Table 2 we have indicated which signals are present or absent in each sample, together with the total number of spins (TNS) from the signals in the disulfide phase.

Influence of Promotor Ions

In Fig. 1 the spectra of standard sulfided Mo(12)/SiO_2, Ni(0.4)–Mo(12)/SiO_2, Ni(4)–Mo(12)/SiO_2, Mo(12)/γ-Al_2O_3, and Ni(4)–Mo(12)/γ-Al_2O_3 are shown. Two signals (II and V) are observable in the spectrum of Mo(12)/SiO_2 (Fig. 1a). It has been shown earlier (*5*) that signals II and V originate from two different paramagnetic sites. Introduction of a small amount of nickel, Ni(0.4)–Mo(12)/SiO_2 (Fig. 1b), leads to an intensity decrease of signal II and a broadening of the left-hand wing of the spectrum. A tenfold increase of the nickel content, Ni(4)–Mo(12)/SiO_2 (Fig. 1c), causes signal II to decrease further. The left-hand wing of the spectrum increases more, possibly caused by the generation of a new signal

TABLE 1

ESR Parameters of the Signals

Signal	Molybdenum			Tungsten		
	Compound	g	ΔH (G)	Compound	g	ΔH (G)
I	$Mo(12)/\gamma\text{-}Al_2O_3$	1.933	80	$W(19.3)/\gamma\text{-}Al_2O_3$	1.78	130
				$Ni(0.4)\text{–}W(19.3)/\gamma\text{-}Al_2O_3$	1.68	300
II	$Mo(12)/SiO_2$	1.985	38	$W(19.3)/\gamma\text{-}Al_2O_3$	1.91	100
				$Ni(0.4)\text{–}W(19.3)/\gamma\text{-}Al_2O_3$	1.91	90
III				$W(19.3)/\gamma\text{-}Al_2O_3$	1.97	50
				$Ni(0.4)\text{–}W(19.3)/\gamma\text{-}Al_2O_3$	1.98	40
IV	$Mo(12)/\gamma\text{-}Al_2O_3$	1.995	68	WS_2	2.01	(180)
				$W(19.3)/SiO_2$	2.00	80
VI	$Ni(4)\text{–}Mo(12)/\gamma\text{-}Al_2O_3$	2.06	220	$Ni(4)\text{–}W(19.3)/\gamma\text{-}Al_2O_3$	2.078	220
				$Ni(4)\text{–}W(19.3)/SiO_2$	2.086	220
				$Co(4)\text{–}W(19.3)/SiO_2$	2.090	320

(VI). Signal V decreases now in intensity. Signal I (oxo-Mo^{5+}) (*5*) reappears and a signal at $g = 1.96$ shows up.

A comparison of the ESR spectra of standard sulfided $Mo(12)/\gamma\text{-}Al_2O_3$ (Fig. 1e) and $Ni(4)\text{–}Mo(12)/\gamma\text{-}Al_2O_3$ (Fig. 1d) clearly shows that signal VI ($g = 2.06$, $\Delta H = 220$ G) is indeed a new signal. Signal II disappears completely and only a trace of signal V remains after introduction of nickel.

The silica-supported molybdenum samples show a higher intensity of signal V than alumina-supported molybdenum catalysts. The TNS hardly changes upon the introduction of promotor ions and is almost independent of the support material. For

TABLE 2

Sample[a]	Total number of spins ($\times 10^{18}$) g^{-1}[b]	Signals[c]					
		I	II	III	IV	V	VI
$Mo(12)/SiO_2$	5.4	VW	VS	–/VW	–/VW	VS	–
$Mo(12)/\gamma\text{-}Al_2O_3$	4.4	S	VS	–/VW	–/VW	S	–
$Ni(0.4)\text{–}Mo(12)/SiO_2$	3.5	VW	VW	–/VW	–/VW	S	W
$Co(0.4)\text{–}Mo(12)/SiO_2$	2.8	VW	W	–/VW	–/VW	S	W
$Ni(4)\text{–}Mo(12)/SiO_2$	3.5	S	VW	–	–	S	S
$Co(4)\text{–}Mo(12)/SiO_2$	3.5	S	W	–	–	S	S
$Ni(4)\text{–}Mo(12)/\gamma\text{-}Al_2O_3$	4.5	S	–	–	–	W	VS
$W(19.3)/SiO_2$	0.8	–	S	–	VW	S	–
$W(19.3)/\gamma\text{-}Al_2O_3$	2.9	–	VS	–/VW	–/VW	S	–
$Ni(0.4)\text{–}W(19.3)/SiO_2$	0.7	–	VW	–/VW	–/VW	S	W/S
$Co(0.4)\text{–}W(19.3)/SiO_2$	0.8	–	W	–/VW	–/VW	S	W/S
$Ni(0.4)\text{–}W(19.3)/\gamma\text{-}Al_2O_3$	2.6	–	W	–	–/VW	S	W/S
$Ni(4)\text{–}W(19.3)/SiO_2$	0.5	–	–	–	–	W	VS
$Co(4)\text{–}W(19.3)/SiO_2$	0.7	–	–	–	–	W	VS
$Ni(4)\text{–}W(19.3)/\gamma\text{-}Al_2O_3$	3.5	–	–	–	–	W	VS

[a] Numbers in parentheses are wt% MoO_3, WO_3, CoO, and NiO, respectively. All samples are sulfided under standard conditions; for details see Experimental section.

[b] Accuracy ±25%.

[c] – = absent; VW = very weak; W = weak; S = strong; VS = very strong.

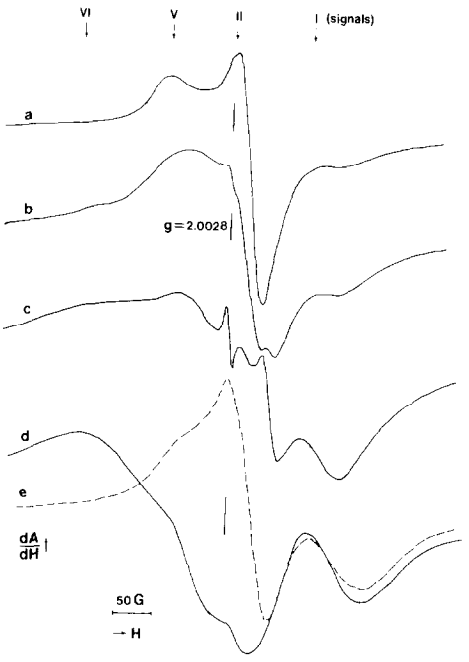

FIG. 1. ESR spectra (recorded at 20 K): (a) $Mo(12)/SiO_2$, receiver gain (RG) 10^2; (b) $Ni(0.4)$–$Mo(12)/SiO_2$, RG 2×10^2; (c) $Ni(4)$–$Mo(12)/SiO_2$, RG 5×10^2; (d) $Ni(4)$–$Mo(12)/\gamma$-Al_2O_3, RG 5×10^2; (e) $Mo(12)/\gamma$-Al_2O_3, RG 10^2. All samples are standard sulfided, for details see Experimental section. Numbers in parentheses are wt% NiO and MoO_3, respectively.

cobalt-promoted $Mo(12)/SiO_2$ catalysts the same observations were made.

The influence of promotor ions on supported sulfided tungsten-containing catalysts is essentially the same as for the molybdenum system. The influence of nickel and cobalt on silica-supported samples is shown in Fig. 2. Increasing the promotor content from 0.4 wt% (Figs. 2b and c) to 4 wt% (Figs. 2d and e) results in a complete disappearance of signal II and a decrease of signal V. Nickel is more effective than cobalt in the breakdown of signal II.

The linewidth of signal VI is larger for cobalt-promoted catalysts. The g-value and linewidth of signal VI are given in Table 1. Comparison of Figs. 2 and 3 (γ-Al_2O_3-supported catalysts) shows that the influence of the promotor (nickel) on the ESR signals of the tungsten system is independent of the support material.

There is, however, a big difference in the TNS between silica- and alumina-supported tungsten-containing catalysts, in contrast to the molybdenum-containing catalysts (see Table 2). The TNS for alumina-supported catalysts is about 5 times larger than that of the silica-supported samples and of the same order of magnitude as for the molybdenum system. The promotor ions have no influence on the TNS.

The tungsten system shows a considerable overlap of signal VI with signal V. The breakdown of signal II is more drastic in the tungsten system than in the molybdenum

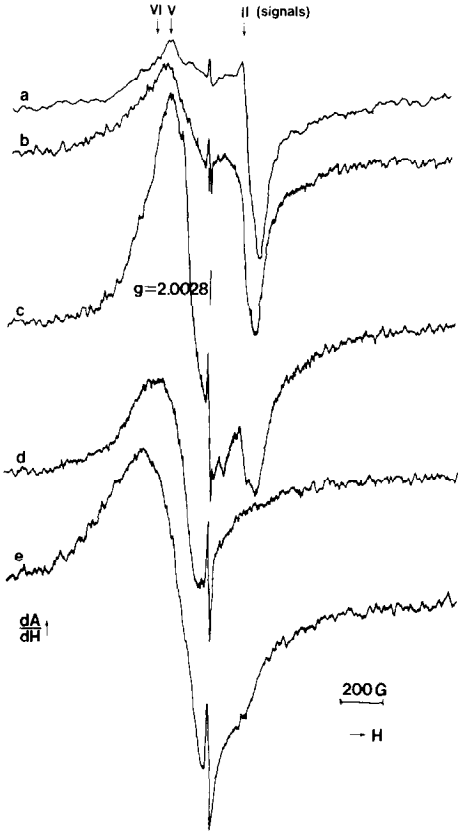

FIG. 2. ESR spectra (recorded at 20 K): (a) $W(19.3)/SiO_2$, RG 5×10^3; (b) $Co(0.4)$–$W(19.3)/SiO_2$, RG 4×10^3; (c) $Ni(0.4)$–$W(19.3)/SiO_2$, RG 4×10^3; (d) $Ni(4)$–$W(19.3)/SiO_2$, RG 4×10^3; (e) $Co(4)$–$W(19.3)/SiO_2$, RG 8×10^3. All samples are standard sulfided. Numbers in parentheses are wt% NiO, CoO, and WO_3, respectively.

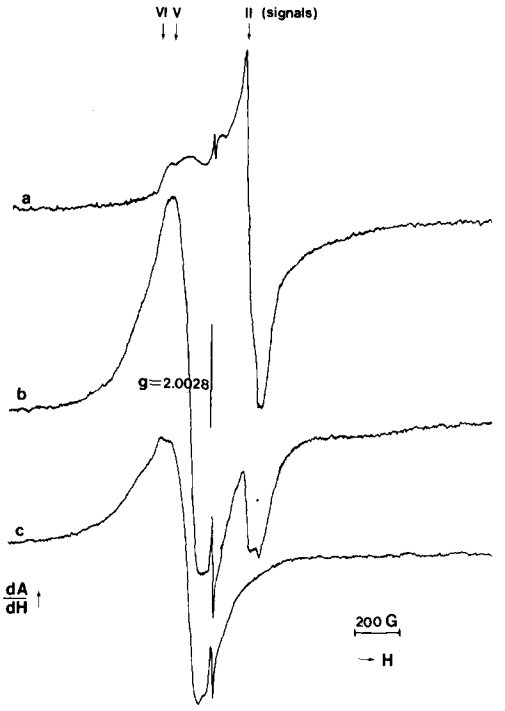

FIG. 3. ESR spectra (recorded at 20 K): (a) $W(19.3)/\gamma\text{-}Al_2O_3$, RG 10^3; (b) $Ni(0.4)\text{–}W(19.3)/\gamma\text{-}Al_2O_3$, RG 10^3; (c) $Ni(4)\text{–}W(19.3)/\gamma\text{-}Al_2O_3$, RG 5×10^2. All samples are standard sulfided.

catalysts. Signal I (oxo-W^{5+}) (5) does not appear in the spectra of tungsten catalysts after introduction of promotor ions.

Effects of Equilibration

In Figs. 4 and 5 the spectra of equilibrated alumina-supported tungsten- and nickel–tungsten-containing catalysts are presented. From Figs. 4a, b, and c ($W(19.3)/\gamma\text{-}Al_2O_3$ equilibrated at H_2S/H_2 = 0.16, 10^{-2}, and 10^{-4}, respectively) it appears that the intensity of signal II decreases with decreasing H_2S/H_2 ratio. In spectrum 4c a signal (III, g = 1.98, ΔH = 40 G) is observable which is the equivalent of signal III detected earlier (5) in $Mo(12)/\gamma\text{-}Al_2O_3$ after treatment of a standard sulfided sample with 7% (v/v) thiophene in helium at 423 K. This signal has not been detected before in the tungsten system. The TNS and the intensity of signal V hardly change after equilibration. For $W(19.3)/SiO_2$ the same effects are observed.

In Figs. 4d and e the spectra of $Ni(0.4)\text{–}W(19.3)/\gamma\text{-}Al_2O_3$ (calcined at 1073 K), standard sulfided and equilibrated at H_2S/H_2 = 10^{-4}, respectively, are given. The effects of equilibration are the same as for the unpromoted catalyst: signal II decreases in intensity and signal III shows up. The g-value resulting from the sum of signals V and VI shifts to a higher value. There is a strong oxo-W^{5+} signal (I) present in these samples due to the high calcination temperature (1073 K, 16 hr).

In Fig. 5 the spectra of equilibrated $Ni(4)\text{–}W(19.3)/\gamma\text{-}Al_2O_3$ are shown. Only

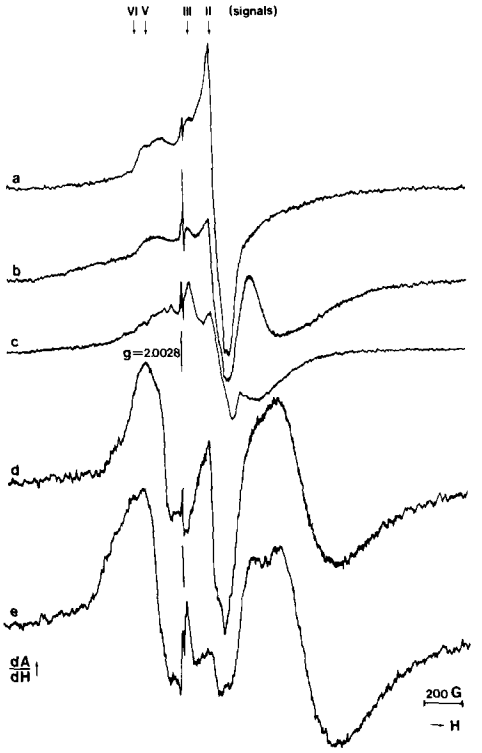

FIG. 4. ESR spectra (recorded at 20 K): (a) $W(19.3)/\gamma\text{-}Al_2O_3$, RG 10^3; (b) $W(19.3)/\gamma\text{-}Al_2O_3$, equilibrated $H_2S/H_2 = 10^{-2}$, RG 10^3; (c) $W(19.3)/\gamma\text{-}Al_2O_3$, equilibrated $H_2S/H_2 = 10^{-4}$, RG 10^3; (d) $Ni(0.4)\text{–}W(19.3)/\gamma\text{-}Al_2O_3$, calcined at 1073 K, standard sulfided, RG 4×10^3; (e) $Ni(0.4)\text{–}W(19.3)/\gamma\text{-}Al_2O_3$, calcined at 1073 K, equilibrated $H_2S/H_2 = 10^{-4}$, RG 4×10^3. For details about the equilibration procedure see Experimental section.

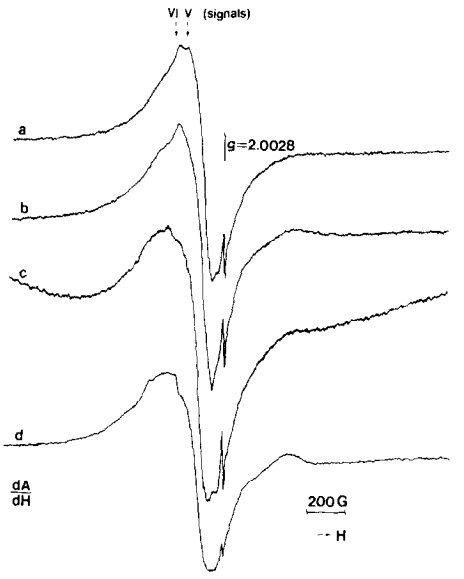

FIG. 5. ESR spectra (recorded at 20 K) of Ni(4)–W(19.3)/γ-Al_2O_3: (a) standard sulfided, RG 5 × 10^2; (b) equilibrated at 673 K, H_2S/H_2 = 10^{-2}, RG 5 × 10^2; (c) equilibrated at 673 K, H_2S/H_2 = 10^{-4}, RG 10^3; (d) equilibrated at 613 K, H_2S/H_2 = 10^{-4}, RG 5 × 10^2.

signals V and VI from the disulfide phase are present. Lowering the H_2S/H_2 ratio leads to a shift of the g-value to a higher value and also the left-hand top of the spectrum shifts to the left (Figs. 5c and d). Signal V seems to diminish and signal VI is converted into a signal with slightly different parameters. Figure 5c, Ni(4)–W(19.3)/γ-Al_2O_3 equilibrated at 673 K with H_2S/H_2 = 10^{-4}, shows a very broad underlying signal which does not appear in the corresponding Ni(0.4)–W(19.3)/γ-Al_2O_3 sample (Fig. 4e) nor in the sample where the equilibration temperature was 613 K (Fig. 5d). The TNS for this catalyst is hardly affected by equilibration.

Effects of CO Adsorption

The vacuum treatment at 295 K did not influence the ESR spectra of W(19.3)/SiO_2 or Ni(4)–W(19.3)/SiO_2. The effect of subsequent CO adsorption at 295 and 473 K is shown in Fig. 6. CO adsorbed on W(19.3)/SiO_2 at 295 K results only in a slight intensity decrease of signal II (Fig. 6b). When CO was adsorbed at 473 K signal II disappeared and a twofold intensity increase of signal IV (ESR parameters after CO adsorption: g = 2.00, ΔH = 80 G) was observed (Fig. 6c). Signal IV was detected earlier (*5*) in bulk WS_2 (g = 2.01 and ΔH = 180 G, values difficult to determine). Subtraction of spectrum 6b from 6c clearly shows that signal IV is the increasing signal.

For Ni(4)–W(19.3)/SiO_2, CO adsorption at 295 K (Fig. 6e) already gives an increase in signal intensity. The parameters of the

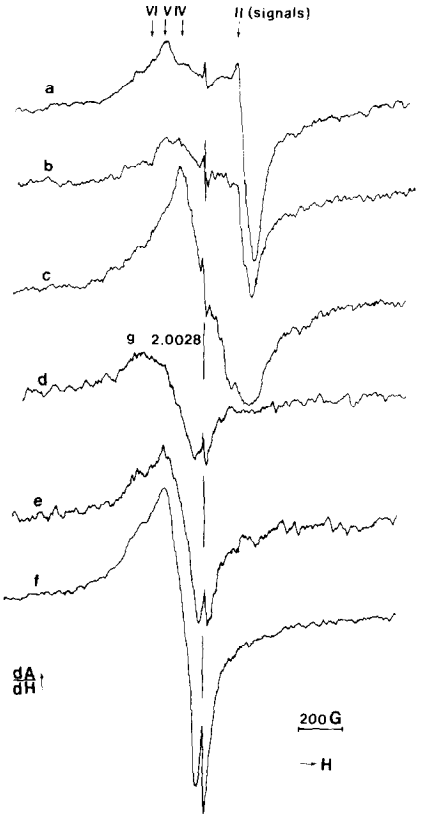

FIG. 6. ESR spectra (recorded at 20 K): (a) W(19.3)/SiO_2, standard sulfided, evacuated at 295 K, RG 5 × 10^3; (b) W(19.3)/SiO_2, standard sulfided +40 Torr CO at 295 K, RG 5 × 10^3; (c) W(19.3)/SiO_2, standard sulfided + 40 Torr CO at 473 K, RG 5 × 10^3; (d) Ni(4)–W(19.3)/SiO_2, standard sulfided, RG 2 × 10^3; (e) Ni(4)–W(19.3)/SiO_2, standard sulfided + 40 Torr CO at 295 K, RG 2 × 10^3; (f) Ni(4)–W(19.3)/SiO_2, standard sulfided + 40 Torr CO at 473 K, RG 10^3. For details about CO adsorption procedure see Experimental section.

signal are slightly different from signal VI (g = 2.060, ΔH = 180 G). When CO is adsorbed at 473 K a sixfold increase of the signal intensity is observed (Fig. 6f). In all cases it is difficult to estimate the contribution of signal V to the signal intensity.

Temperature Dependence of the Signal Intensity

In Fig. 7 the reciprocal signal intensity (double integration of the spectrum without signal I) versus the temperature is plotted for standard sulfided $W(19.3)/SiO_2$ and $Ni(4)–W(19.3)/SiO_2$. The temperature region for which the Curie–Weiss law holds is 20–200 K for $W(19.3)/SiO_2$ and 20–100 K for $Ni(4)–W(19.3)/SiO_2$. Molybdenum-containing catalysts show the same behavior. In this region the TNS has been calculated.

Activity Measurements

Thiophene HDS and butene hydrogenation activity data are listed in Table 3. The reaction rate for thiophene HDS has been calculated on the basis of a pseudo-first-order reaction in thiophene. The hydrogenation to butane of the butenes formed upon HDS, is expressed as percentage butane over butenes + butane (insufficient data for reaction rate determination).

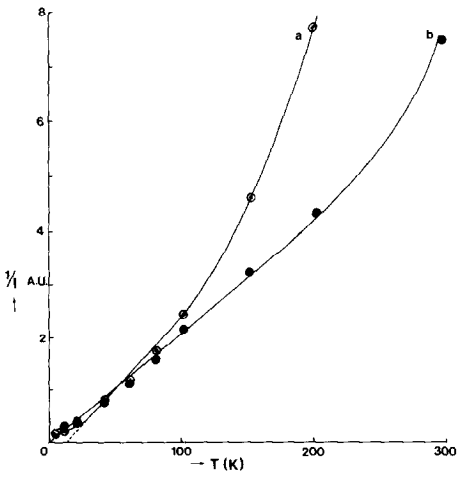

FIG. 7. Temperature dependence of the signal (II–VI) intensity. (a) $Ni(4)–W(19.3)/SiO_2$; (b) $W(19.3)/SiO_2$. Standard sulfided samples.

TABLE 3

Catalytic Activities[a]

Sample	$r^b \times 10^3$ HDS (mole hr^{-1} g^{-1})	Hydrogenation to butane (%)
$Mo(12)/SiO_2$	8.9	16
$Mo(12)/\gamma\text{-}Al_2O_3$	8.4	19
$Ni(4)–Mo(12)/SiO_2$	35.9	8
$Co(4)–Mo(12)/SiO_2$	29.4	8
$Ni(4)–Mo(12)/\gamma\text{-}Al_2O_3$	30.3	25
$W(19.3)/SiO_2$	3.8	7
$W(19.3)/\gamma\text{-}Al_2O_3$	2.8	9
$Ni(0.4)–W(19.3)/SiO_2$	18.0	7
$Ni(0.4)–W(19.3)/\gamma\text{-}Al_2O_3$	3.3	12
$Ni(4)–W(19.3)/SiO_2$	25.3	6
$Ni(4)–W(19.3)/\gamma\text{-}Al_2O_3$	28.6	12

[a] For test conditions see Experimental section.
[b] $r = -(F/W)\ln(1 - x) = -0.045\ln(1 - x)$.

The thiophene HDS activity is enhanced by a factor of 3–10 as a result of the addition of promotor ions. For tungsten-containing catalysts the promoting effect is more pronounced than for the molybdenum system. The technique of "double" sulfiding makes it possible to prepare silica-supported catalysts with HDS activities comparable with alumina-supported catalysts. The catalytic activity of alumina-supported catalysts is not enhanced by addition of a small amount of promotor ($W(19.3)/\gamma\text{-}Al_2O_3$, $r = 2.8 \times 10^{-3}$; $Ni(0.4)–W(19.3)/\gamma\text{-}Al_2O_3$, $r = 3.3 \times 10^{-3}$) whereas the corresponding silica-supported catalysts show a fivefold increase of activity ($W(19.3)/SiO_2$, $r = 3.8 \times 10^{-3}$; $Ni(0.4)–W(19.3)/SiO_2$, $r = 18 \times 10^{-3}$).

Although no reaction rate could be determined for the hydrogenation to butane it appears that for catalysts without promotor the hydrogenation activity is independent of the support. The alumina-supported promoted catalysts show a two- to threefold-higher hydrogenation activity than the silica-supported samples.

DISCUSSION

Influence of Promotor Ions on the ESR Spectra

Let us first summarize the results of the previous section. Introduction of a small

amount of promotor (Ni(Co)/W(Mo) = 0.064 atomic ratio) causes a decrease of signals II, III, and V but they are still present or can be generated by a proper treatment (low H_2S/H_2 ratio → signal III). Signal IV seems to disappear completely and cannot be generated by equilibration or evacuation. (In unpromoted catalysts the intensity of signal IV increased after evacuation of the sample at 673 K (*5*).) The broadening of the left-hand wing of the spectrum points to the formation of a new signal VI. A tenfold increase of the promotor content leads to complete disappearance of signals II, III, and IV (they do not show up after equilibration or evacuation) in Ni(4)–Mo(12)/γ-Al_2O_3 and the tungsten-containing catalysts. Only signals V and VI are present and especially for the tungsten system it is difficult to estimate the intensity of each signal. The samples Ni(Co)(4)–Mo(12)/SiO_2 still contain traces of signals II and III but the main contributors to the TNS are signals V and VI.

Since signals II, III, and IV are attributed to paramagnetic sites at the edge surface of the disulfide crystals (*5*), the results mentioned above are explained by a surface reorganization due to the incorporation of promotor ions in the edges of the disulfide crystals. Farragher and Cossee (*3*) proposed the decoration model to explain the increase in benzene hydrogenation activity of WS_2 after addition of small amounts of nickel. The basic idea of this model is a surface reorganization due to a filling of the octahedral holes between the disulfide layers with nickel as Ni^{2+} ions, accompanied by an electron transfer from zerovalent nickel to W^{4+} ions: $Ni^0 + 2W^{4+} \rightarrow Ni^{2+} + 2W^{3+}$. This process is restricted to the edge surfaces for WS_2 and MoS_2 (d^2 configuration) since the d-orbital splitting of W^{4+} (Mo^{4+}) in D_{3h} symmetry forbids the accommodation of an additional electron. The model is in accordance with the fact that nickel and cobalt influence the ESR spectra of supported sulfided molybdenum and tungsten catalysts essentially in the same way, as is expected from the strong similarity between the crystal parameters of WS_2 and MoS_2 as well as between the ionic radii of Ni^{2+} and Co^{2+}.

It is remarkable that the linewidth and g-value of signal VI for promoted molybdenum and tungsten catalysts are almost the same whereas there are large differences between the ESR parameters of the signals in the unpromoted catalysts (see Table 1). The expressions for the g-values are determined by the symmetry of the ligand field. The spin–orbit coupling parameter λ and the energy difference Δ between the d-orbital levels are determined by the nature of the ions and the lattice parameters. For signals indicated with the same number the corresponding ligand-field symmetry is expected to be the same. Different g-values for corresponding signals in molybdenum and tungsten catalysts are thus caused by different values for λ and/or Δ. The spin–orbit couplings of Mo and W d-electrons differ and are quite large (λ = 0.11 and 0.28 eV for free Mo^{4+} and W^{4+} ions, respectively (*10*)). In solids the value of λ is between 0.50 and 0.85 of the free-ion value (*11*). For MoS_2 λ = 0.09 has been calculated (*12*). The larger value of λ for tungsten compared with molybdenum together with different Δ values can explain the larger deviation from g = 2.0023 for the g-value of signals I and II in tungsten-containing catalysts. The g-value of signal VI (2.06 for Mo and 2.084 ± 0.006 for W) clearly shows that nickel (cobalt) has a very pronounced influence on the paramagnetic centers. Possibly, incorporation of nickel causes a change in Δ values of superexchange between nickel and W (Mo) occurs.

The linewidth of ESR signals in these samples might be and most probably is determined by dipole–dipole interactions. The linewidth of signal VI seems to depend only on the nature of the promotor ion (ΔH = 220 G for nickel-promoted catalysts and 320 G for cobalt-promoted samples). The linewidth of the other ESR signals is independent of the presence or absence of pro-

motor ions. The difference in g-value of signal VI for Mo- or W-containing catalysts, together with the fact that signal VI has never been detected in samples containing only promotor ions, leads to the conclusion that the electron giving rise to this signal is primarily located on Mo or W ions.

Since the Curie temperatures of the samples are different it is necessary to calculate the TNS from the reciprocal intensity versus temperature curves. For paramagnetic ions for which the Curie–Weiss law holds, the magnetic susceptibility is

$$I = \frac{g^2\beta^2(\mathrm{TNS})S(SH)}{3k(T - \theta)}. \qquad (1)$$

It has been assumed that for all samples the effective spin value $S = \frac{1}{2}$. From Eq. (1) one can deduce that the TNS is proportional to $1/g^2 tg\ \alpha$ (α is the angle between the $1/I$ versus T curve in the Curie–Weiss region of Fig. 7). Calibration of the absolute number of spins has been performed by applying this procedure to a Varian Strong Pitch sample. The observed deviations from the Curie–Weiss law in the high-temperature region can be supposed to be caused by a loss of electrons to a higher energy level, for instance the conduction band. The ratio between the electrons in both levels is $N_2/N_1 = Ze^{-\Delta\epsilon' kT}$ ($\Delta\epsilon$ is the energy difference between level 2 and level 1, and Z is the ratio between the density of states of level 2 and level 1). When $\Delta\epsilon$ changes, the temperature domain in which the Curie–Weiss law is obeyed will change. For promoted catalysts this domain was found to be smaller which means that $\Delta\epsilon$ was smaller. For two catalysts, Ni(4)–W(19.3)/SiO_2 and Ni(4)–W(19.3)/γ-Al_2O_3, the data available were sufficient to permit a calculation of Z and $\Delta\epsilon$ with an estimated accuracy of 50%. The values are $Z = 100$, $\Delta\epsilon = 0.07$ eV for silica-supported and $Z = 15$, $\Delta\epsilon = 0.04$ eV for alumina-supported catalyst. The value of Z will be influenced by the size of the disulfide crystals, since only edge atoms contribute to N_1 while all crystal atoms have to be taken into account for N_2. For the silica-supported samples larger crystals are expected since silica is more inert than alumina, which is in accordance with the Z-values. From the $\Delta\epsilon$-values it appears that the W^{3+} ions form a donor level most probably just below the conduction band. The present data are not accurate enough to determine whether the difference in $\Delta\epsilon$-values is real or just within experimental error.

For tungsten-containing catalysts the difference in Z-values is accompanied by a difference in TNS. A low Z-value gives rise to a high TNS. For molybdenum-containing catalysts lack of data prohibited the calculation of Z-values. It is remarkable, however, that the TNS for alumina- and silica-supported catalysts are of the same magnitude.

The values obtained above for TNS, $\Delta\epsilon$, and Z are overall values (the sum of signals II–VI). It is difficult to estimate the contribution of each signal, especially for the broader signals IV–VI. Although the TNS hardly changes after introduction of promotor ions it is clear that the contributing paramagnetic species do change. The surface sites II, III, and IV disappear and VI is formed. Site V, possibly originating from bulk defects, diminishes which could point out a neater crystallization upon introduction of promotor ions. The overlap of signal V with signal VI hampers a quantitative interpretation of the different support dependence of the TNS for molybdenum- or tungsten-containing catalysts. For the molybdenum-containing catalysts it is clear that for Ni(Co)(4)–Mo(12)/SiO_2(γ-Al_2O_3) signal VI is the main contributor (>75%) to the TNS. The low TNS values for silica-supported tungsten-containing catalysts could be due to larger crystallites compared to alumina-supported samples since silica is a more inert support. The crystallite size and the number of defect structures for molybdenum-containing catalysts are possibly less support dependent. In this re-

spect it is noteworthy that for MoS_2 a poorly crystalline structure is known (*14*).

It is interesting to compare the above results with data reported by Voorhoeve for tungsten-containing catalysts (*7*). He reported a 10- to 100-fold increase in the TNS as a result of introducing nickel in alumina-supported and bulk WS_2.

The main differences between the present study and Voorhoeve's work have to be found in the ESR spectra of the unpromoted catalysts. The spectra presented here are more complex and probably contain a larger contribution due to bulk defects. The different sulfiding procedure applied here (lower sulfiding temperature, atmospheric pressure) might be the cause of these differences.

Influence of Equilibration upon the ESR Spectra

The results obtained with equilibration have to be compared with the evacuation experiments at 673 K with unpromoted catalysts presented earlier (*5*). While equilibration leads to an intensity decrease of signal II and an increase of signal III, evacuation leads to an intensity decrease of signal II and an increase of signal IV, which is not affected by equilibration. Konings *et al.* (*5*) suggested some configurations of atoms at the edges of disulfide crystals, and possible valence and/or symmetry changes upon adsorption and desorption of H_2S in the form of S^{2-} or SH^- were given. The combined information from equilibration and vacuum treatment experiments makes it possible to rationalize better the nature of the paramagnetic centers that give rise to the various signals. Depending on whether one deals with a $(10\bar{1}0)$ or a $(\bar{1}010)$ surface (*5*, *15*) two series of surface atom configurations are possible (see Fig. 8). In the $(10\bar{1}0)$ surface every metal ion has four sulfur ligands that are shared with two other metal ions and two anion coordination sites of its own, while in the $(\bar{1}010)$ surface two sulfur ligands are shared with two other metal ions and four anion coordination sites are shared with one other metal ion.

The edges of the disulfide crystals consist of an alternate stacking of $(10\bar{1}0)$ and $(\bar{1}010)$ surfaces. The doubly shared and single-coordination sites can be vacant or filled with S^{2-} or SH^- ions. Since signal IV grows upon evacuation and is not sensitive to equilibration it will be associated with surface configurations containing vacancies and sulfur ligands, for instance $M^{3+}S_4\square_2$. Signals II and III that disappear upon evacuation and are sensitive to equilibration originate from paramagnetic centers in which several or all vacancies are filled. Most probably type II centers are metal ions, fully coordinated, mainly with S^{2-} ligands, while type III centers may have some vacancies and the other coordination sites filled with SH^- groups.

For samples with low promotor content (0.4 wt%) type IV centers are absent and types II and III are the same as for unpromoted catalysts. It is difficult here to draw conclusions about signal VI since signal V (insensitive to evacuation or equilibration) strongly interferes.

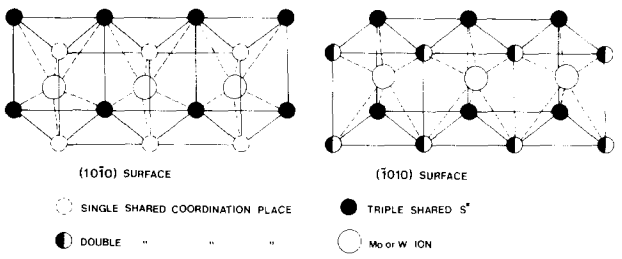

FIG. 8. Edge structure of WS_2 (MoS_2) crystals.

Samples with a high promotor content (4 wt%) do show a slight change in their ESR spectra upon equilibration. Inspection of Fig. 9 shows that site type VI also has the possibility of having vacancies, S^{2-}, or SH^- ions on the double-coordination sites. Increase of SH^- ligands over S^{2-} could cause the slight change in ESR parameters.

Voorhoeve (*7*) reports a strong intensity increase of the ESR signals in promoted catalysts when the H_2S/H_2 ratio is lowered. It is argued that the lower the H_2S/H_2 ratio is, the more vacancies there are, which should lead to more W^{3+} ions. From the model proposed above it appears that there is no need for a correlation between the H_2S/H_2 ratio and the number of W^{3+} ions, since adsorption of H_2 and the formation of SH groups will change the tungsten ion valency. Probably different sample conditioning before recording the ESR spectra (evacuation at higher temperatures?) can account for the differences between Voorhoeve's results and the present study.

The formation of metallic nickel observed at $H_2S/H_2 = 10^{-4}$ and 673 K (see Fig. 5c) is in accordance with the phase diagram of nickel sulfide in H_2S/H_2 atmosphere (*16*).

Influence of CO Adsorption upon the ESR Spectra

The intensity decrease of signal II (sulfo-W^{5+}) and the increase of signals IV and VI (sulfo-W^{3+}) can be explained by an electron donation to tungsten ions as a result of CO adsorption. This is in accordance with earlier findings (*5*): signal II decreases after evacuation at 673 K and after reduction with hydrogen, signal IV increases after evacuation at 673 K. The decrease of signal IV after reduction with hydrogen could be caused by overreduction to W^{2+}.

Carbon monoxide has electron-donor properties and direct electron transfer from CO to tungsten or indirect via a decorating nickel ion is a possible reaction. Another possibility is the formation of COS, a reaction that is known to take place over transition metal sulfides (*17*). This reaction would lead to the donation of electrons:

$$CO + S^{2-} \rightarrow COS_{ads} + 2e.$$

For the unpromoted catalyst the sulfur ions involved in this reaction can only be supplied by the WS_2 phase whereas for the promoted catalyst the reaction may also take place over a separated nickel sulfide phase followed by electron transfer to the WS_2 phase via conduction. An indication for CO adsorption on WS_2 is the observation that the parameters of the ESR signal from the disulfide phase are slightly changed after CO adsorption.

In the presence of nickel an increase in signal intensity after CO adsorption is observed already at 295 K while the unpromoted sample has to be heated to 473 K. In this respect it is noteworthy that especially nickel sulfide and cobalt sulfide have a high activity for the formation of COS (*17*). These findings suggest that CO adsorption may very well occur on a sulfur ion belonging to the coordination sphere of both a tungsten ion and a decorating nickel ion in case of Ni(4)–W(19.3)/SiO_2. Such a sulfur ion would possibly more easily form COS and donate electrons to the disulfide phase.

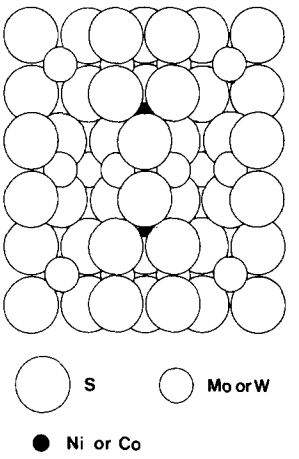

FIG. 9 {10$\bar{1}$0} surface of WS_2 (MoS_2), with ideal ordered surface sulfur due to decoration by Ni or Co.

Activity Measurements

As shown in the literature (*8, 18*), providing the proper preparation method is applied, highly active HDS catalysts can be prepared on different types of support materials. This is a strong argument for models that ascribe the HDS activity to the presence of the disulfide phase in contrast to the monolayer model, molybdenum with oxygen and sulfur ligands (*19, 20*).

For silica-supported tungsten catalysts a small amount of nickel (Ni/W = 0.07 atomic ratio) already gives a drastic HDS activity increase. It was found (*21*) that the thiophene HDS activity increases linearly with the Ni/W atomic ratio in the range 0–0.1 and then stays constant with a decrease at very high nickel contents. This linear increase and saturation at low Ni/W ratio is in accordance with the decoration model (*3*) while the synergism model (*4*) predicts a saturation at much higher promotor levels. From the Ni/W ratio at which the level of constant HDS activity is reached, the size of the WS_2 crystallites can be calculated if it is assumed that the decoration model is valid. Figure 9 shows a stoichiometric $\{10\bar{1}0\}$ edge with a sulfur atom ordering that is assumed to be most ideal for benzene hydrogenation (*3*) and thiophene HDS. One-quarter of the octahedral holes between the disulfide layers are filled with promotor ions, stabilized by six sulfur ligands in this configuration. The number of octahedral holes equals the number of edge tungsten ions (W_e), which is related to the total number of tungsten ions (W_t) by: $W_e/W_t = 1.26/d$ (d is the crystal diameter perpendicular to the C axis in nm). Thus $\bar{d}$ = 0.315 × optimum tungsten/nickel atomic ratio.

For the Ni–W/SiO_2 system a crystallite size of 3.15 nm is thus calculated. This is a very reasonable value and thus in support of the decoration model. In practice there will always be additional promotor ions attached to the carrier and probably in octahedral holes without full sulfur coordination. The calculated value must therefore be regarded as a minimum.

For alumina-supported catalysts the promotor–support interaction prevents the first small amount of promotor ions from decorating the disulfide phase, which explains the equal HDS activities of W(19.3)/γ-Al_2O_3 and Ni(0.4)–W(19.3)/γ-Al_2O_3.

A correlation between thiophene HDS activity or butene hydrogenation activity and the intensity of one of the ESR signals observed, has not been found yet. It is, however, possible that signal VI correlates with the thiophene HDS activity. This signal is absent in unpromoted catalysts, and is the main signal in samples with 4 wt% promotor. As discussed before its intensity in samples with 0.4 wt% promotor is difficult to estimate because of strong overlap with signal V. Future research will be directed to the preparation of catalysts with low signal V intensity, possibly by sulfidation under higher pressure (±10 atm), and catalyst activity tests under medium high pressure.

CONCLUSIONS

The main conclusions of the present work are:

i. Incorporation of nickel or cobalt in supported tungsten- or molybdenum-containing catalysts influences the ESR spectra in a similar way. The results can be best understood in terms of a decoration model.

ii. The intensities of signals II, III, IV, and VI are dependent on the composition of the interacting atmosphere (i.e., equilibration in H_2S/H_2 mixtures, and/or CO adsorption, and/or vacuum treatment). The corresponding paramagnetic centers are most likely situated at the edges of the disulfide crystals.

REFERENCES

1. Voorhoeve, R. J. H., and Stuiver, J. C. M., *J. Catal.* **23**, 228 (1971).
2. Amberg, C. H., *J. Less-Common Metals* **36**, 339 (1974).

3. Farragher, A. L., and Cossee, P., *in* "Proceedings, 5th International Congress on Catalysis, Palm Beach, 1972" (J. W. Hightower, Ed.), p. 1301. North-Holland, Amsterdam, 1973.
4. Hagenbach, G., Courty, Ph., and Delmon, B., *J. Catal.* **31,** 264 (1973).
5. Konings, A. J. A., Van Dooren, A. M., Koningsberger, D. C., de Beer, V. H. J., Farragher, A. L., and Schuit, G. C. A., *J. Catal.* **54,** 1 (1978).
6. Van der Aalst, M. J. M., and de Beer, V. H. J., *J. Catal.* **49,** 247 (1977).
7. Voorhoeve, R. J. H., *J. Catal.* **23,** 236 (1971).
8. de Beer, V. H. J., Van der Aalst, M. J. M., Machiels, G. J., and Schuit, G. C. A., *J. Catal.* **43,** 78 (1976).
9. de Beer, V. H. J., Van Sint Fiet, T. H. M., Engelen, J. F., Van Haandel, A. C., Wolfs, M. W. J., Amberg, C. H., and Schuit, G. C. A., *J. Catal.* **27,** 357 (1972).
10. Herman, F., and Skillmann, S., "Atomic Structure Calculations." Prentice-Hall, Englewood Cliffs, N.J., 1963.
11. Owen, J., and Thornley, J. H. M., *Rep. Progr. Phys.* **29,** 675 (1966).
12. Title, R. S., and Shafer, M. W., *Phys. Rev. Lett.* **28,** 808 (1972).
13. Wentrcek, P. R., and Wise, H., *J. Catal.* **51,** 80 (1978).
14. Chianelli, R. F., Prestridge, E. B., Pecararo, T. A., and DeNeufville, J. P., *Science* **203,** 1105 (1979).
15. Farragher, A. L., *Advan. Colloid Interface Sci.* **11,** 3 (1979).
16. Weisser, O., and Landa, S., "Sulphide Catalysts: Their Properties and Applications," p. 47. Pergamon, New York, 1973.
17. Fukuda, K., Dokiya, M., Kameyama, T., and Kotera, Y., *J. Catal.* **49,** 379 (1977).
18. Stevens, G. C., and Tennison, S. R., British Patent 1,471,588 (1977).
19. Schuit, G. C. A., and Gates, B. C., *AIChE J.* **19,** 417 (1973).
20. Massoth, F. E., *J. Catal.* **36,** 164 (1975).
21. Konings, A. J. A., to be published.